Digital restoration of ancient color manuscripts from geometrically misaligned recto-verso pairs

Abstract

We propose a fast automatic procedure for registration and restoration of images of recto-verso pairs of color manuscripts affected by bleed-through distortion. The registration algorithm assumes a rigid projective deformation of a side with respect to the other. The coefficients of the geometric transformation are computed from a large number of pairs of matching points, automatically detected by exploiting the estimates of local shifts between pairs of small patches. We validate the efficiency of the registration algorithm through the performance of a restoration method based on a model that relates each couple of corresponding pixels in the two images, and thus requiring a very accurate alignment of the two sides. The experiments show that this combined procedure of registration plus restoration can provide an excellent removal of the bleed-through pattern, while leaving unaltered the salient features of the original manuscript.

1 Introduction

The most frequent degradation affecting ancient manuscripts written on both sides of the page is bleed-through, caused by the seeping of the ink through the paper fiber. This makes the text of the reverse side to interfere with the foreground text, thus making fatiguing and tedious the work of scholars when reading or transcribing the manuscript. This damage persists in the digital acquisitions becoming a standard in archives, museums and libraries, for conservation and fruition scopes. Even scanned modern documents may present a similar degradation caused by light transmission (show-through), which may seriously downgrade the performance of OCR.

Physical restoration of such manuscripts is impossible, since the chemical substances needed would also destroy the ink of the foreground text. Digital (or virtual) restoration thus represents the only viable way to remove or attenuate these interferences from the digital versions of the manuscripts, usually exploiting both sides, called recto and verso.

In [1], the Chan-Vese active contour model is modified to incorporate recto-verso information, and then a function minimization technique corrects the strokes cancelled where the two texts overlap. In [2], to classify the pixels as foreground, bleed-through or background, a regularized energy function is defined that uses as data term likelihoods derived from small sets of user-labeled pixels, and as smoothness term a dual-layer Markov Random Field (MRF). A 4-class classification approach is proposed in [3], by segmenting the recto-verso joint histogram with the aid of available ground truths. Pixel misclassifications are then iteratively corrected by analyzing the connected components in the segmented image, and the bleed-through regions are inpainted with background patterns.

In other works, recto and verso are modeled as two parametric mixtures of the uncorrupted front and rear sides, to be recovered by blind or semi-blind source separation techniques. Linear models lead to fast algorithms, based on Independent Component Analysis (ICA) or data decorrelation [4] [5]. Compensations for the apparent non-linearity and/or non-stationarity of the physical phenomenon have been attempted by MRF-based regularization [6][7], or penalized Non-negative Matrix Factorization [8]. The non-linear convolutional model derived in [9] for show-through inspired the work in [10], where the non-linearity is assumed known, and the problem is regularized by total variation. In [11] and [12], we experimented the same model for bleed-through, employing either fully blind constrained maximum likelihood, or off-line estimation of the model parameters. For show-through, in [13] a quadratic convolutional model is solved through maximum likelihood, and in [14] the parameters of a non-linear but invertible model are learned by non-linear ICA. In [15], non-linear diffusion and wavelet transforms are used to model and remove bleed-through. Finally, in [16] a non-stationary model, linear in the optical densities, is experimented.

Since the above techniques are very sensitive to even slight misalignments of the two sides, a very accurate registration of the recto and verso images must be performed prior restoration.

To digitally acquire ancient manuscripts, usually professional cameras are used, either high resolution CCD cameras or multispectral cameras, mounted on special mechanical equipments that guarantee a stable setup. Despite that, misalignments between the images of the two sides are likely to occur, due to the human intervention needed for turning around and repositioning the leaf. Registration of recto-verso images is not an easy task, since the intensity of corresponding foreground and bleed-through areas are usually very different, bleed-through might only occur sparsely across the page, and the binding of the page in case of books may have different degree of curvature in the two sides.

General-purpose image registration techniques are surveyed in [17], whereas [18] overviews methods based on mutual information, with application to medical images. Registration methods specifically designed for recto-verso pairs considered initially global and rigid affine transformations, whose parameters are estimated by minimizing the intensity differences between the two sides [19], or, as in [20], through an improved, but computationally intensive, version of the point pattern matching method [21] using local features and local searching strategies. In [22], a first step of coarse alignment exploits the correspondence of two "anchors" extracted from the two sides. Then the recto is further matched with the verso using a block-by-block strategy, where for each block on the recto the corresponding patch on the verso is searched for in a larger window, by spatial cross-correlation. Since block-based alignment produces "holes", a radial basis function technique is used to recover lost information. In [23] we proposed using the Fourier-Mellin transform, whereas, for printed documents, in [24] the rotation angle is estimated from the recto bleed-through profile, and the vertical and horizontal translations are estimated from profiles of both the verso foreground and the recto bleed-through. Projective transformations have also been proposed, e.g. in [25], where a feature-based method first detects the character contours, and then uses the contour corners.

A non-rigid registration method is proposed in [26], where a global affine transformation is combined with a free-form, hierarchical transformation model based on B-splines and detected recto and verso corresponding control points. A thin plate spline smoothness constraint is applied for minimizing the residual complexity between the two sides, as done in [27]. However, strong bleed-through is required to locate correspondences between bleed-through and foreground. In [28], a similar method is proposed, where the two sides are first globally aligned using the page outline, and then a local grid point warp is applied combining the norm of differences between both intensity and gradient with a content preserving smoothness penalty.

In this paper we consider flat manuscripts (e.g. letters), so that we assume a global rigid deformation of the horizontally reflected verso with respect to the recto. However, we extend the transformation to be projective, since, besides translations and rotation caused by turning around the leaf, accidental movements of the camera (e.g., a small pitching moment), may also cause scale changes and projective deformations.

We estimate the transformation parameters by least mean squares (LMSE), based on a suitable number of corresponding points in the two images. Rather than searching for matching points among the set of singular points, such as corners or crosses, they are automatically detected by looking at the maximum of the cross correlation between small patches of same size and same location in the two sides. In other words, the center of each recto patch is assumed to correspond to that verso point having the coordinates of the peak of the cross correlation function. Reasonably assuming a moderate misalignment at local level enables performing this estimation by exploiting the shift property of the Fourier Transform (FT), through the computation of the cross power spectrum of the two patches. Using FFT, this computation is very fast, allowing the quick detection of a very large number of relative translations and then corresponding points, which makes more robust LMSE.

Since we consider RGB manuscripts, the subsequent restoration procedure can be performed by applying separately to each pair of recto-verso color channels any of the available algorithms for see-through removal from recto-verso grayscale manuscripts, and then recomposing the restored channels to obtain the restored RGB sides. Note however that, to preserve the original RGB appearance of the manuscript, the restoration algorithm must satisfy precise conditions. Just to mention two aspects, a pixel should be recognized as background, foreground or see-through in all the three color planes, and the graylevel range of each color plane must be conserved. Hence, for instance, an algorithm that provides an almost binary result is not suitable for color preservation purposes. In [16] we proposed a restoration algorithm for grayscale recto-verso pairs that possesses the requested properties.

This algorithm is based on a data model where the observed optical density of each side is given by the linear combination of the density of the undegraded side and an ink-smeared version of the ideal density of the opposite side, weighted by a pixel-dependent positive parameter, which represents the degree of attenuation of the text that shines through. Based on simple considerations, these interference levels are estimated from the data, and the data model is then inverted in a single step, making the algorithm very fast.

The algorithm is able to remove only the unwanted interferences, while preserving other patterns, such as stamps or pencil annotations, that are peculiar of each side, as well as the original colors of foreground and background.

The paper is organized as follows. In Section 2, the projective registration method is described. Section 3 summarizes the model-based algorithm for bleed-through removal, while Section 4 is devoted to experimental results on ancient color manuscripts, either acquired through a high resolution CCD camera or a multispectral camera. In Section 5 we analyze the performance of the method, and, finally, Section 6 concludes the paper with possible improvements and extensions.

2 The registration method

Depending on the acquisition device, we distinguish two cases. In CCD cameras, the three Red, Green and Blue channels $r_c(i,j)$ and $v_c(i,j)$, $c = \{R, G, B\}$ of each side are aligned, so that we can consider the same projective transformation for the three pairs of homologous channels. Professional multispectral cameras acquire instead separately the three color channels, by using different filters, often causing the further misalignment between the color planes. Color shift correction, necessary for any kind of analysis of the manuscript, is even more critical when comparing recto-verso pairs, since, due to the horizontal reflection of one of the images, the misalignment of the color planes is "inverted" in the two images. Among the various possible strategies, we chose to first align the recto color planes and then geometrically register the two sides through the application of three different projective transformations, one for each pair of color channels.

Let us first assume the perfect alignment of the color planes. If (x, y) and $(x + \Delta x, y + \Delta y)$ are two geometrically corresponding locations of the recto and verso sides of the physical manuscript, a projective transformation between the two locations, unique for the three pairs of homologous channels, has a form like the following one:

$$\begin{bmatrix} x + \Delta x \\ y + \Delta y \\ 1 \end{bmatrix} = \begin{bmatrix} s_x \cdot cos(\theta) + p_x b_x & -s_y \cdot sin(\theta) + p_y b_x & b_x \\ s_x \cdot sin(\theta) + p_x b_y & s_y \cdot cos(\theta) + p_y b_y & b_y \\ p_x & p_y & 1 \end{bmatrix} \begin{bmatrix} x \\ y \\ 1 \end{bmatrix} \quad (1)$$

where homogeneous coordinates are used, b_x and b_y, s_x and s_y, p_x and p_y represent translations, scale factors and projective deformations, respectively, along the x and y axes, and θ is the angle of rotation. Thus, given the digital images $v_c(i,j)$, $c = \{R, G, B\}$ of the verso, their versions registered on the recto will be built by applying to each pixel (i,j) of a ordered grid the transformation above, and then computing its graylevel by interpolating the values of those pixels that, in the original verso, surround the possibly non-integer location so found. In this work, we adopted bicubic interpolation.

To determine the seven parameters of the transformation in eq.(1) by using LMSE, a minimum of four pairs of corresponding locations are needed. Of course, a larger number of pairs will ensure more accurate estimates, since possible small mismatches of the corresponding locations can be compensated.

In general, automatically finding homologous pixels in recto-verso images affected by see-through is not easy, since corresponding strokes may have very different intensities, or even be absent in one of the two sides. The strategy we adopt is based on the shift property of the FT, exploited to determine the relative displacements of a large number of pairs of small patches selected, at the same position, from the original recto and verso images. The patches must have the following properties: i) whole background areas should be avoided; ii) they must be small enough to assume that their misalignment can be approximated by a translation only; iii) they must be large enough to share a common portion of text. This last requirement, though implying a moderate deformation between the two sides, is not too strict, since the acquisitions of historical manuscripts are usually done with accuracy.

Given two patches f_1 and f_2 such that, in a common support, it is $f_1(x + \Delta x_0, y + \Delta y_0) = f_2(x, y)$, the following relationship between their FTs holds true:

$$F_2(\omega_x, \omega_y) = F_1(\omega_x, \omega_y) e^{j(\omega_x \Delta x_0 + \omega_y \Delta y_0)} \tag{2}$$

from which:

$$\frac{F_2(\omega_x, \omega_y)}{F_1(\omega_x, \omega_y)} = e^{j(\omega_x \Delta x_0 + \omega_y \Delta y_0)} \tag{3}$$

Then, theoretically, the inverse FT of the ratio in eq. (3) will return a delta of Dirac impulse located in $(\Delta x_0, \Delta y_0)$. Nevertheless, as always happens when inverse filtering is used, due to the presence of random noise, dissimilar parts and gain changes, this operation produces a very noisy map, where a trustable peak cannot be located. A more robust estimate of the cross correlation between f_1 and f_2 is given by the inverse FT of the cross power spectrum:

$$\frac{F_2(\omega_x, \omega_y) \cdot F_1^*(\omega_x, \omega_y)}{|F_2(\omega_x, \omega_y)| \cdot |F_1^*(\omega_x, \omega_y)|} = e^{j(\omega_x \Delta x_0 + \omega_y \Delta y_0)} \tag{4}$$

where $*$ denotes the complex conjugate. The location of the now well emerging peak of the cross correlation function so computed defines the relative displacement between the two patches. Once the displacement is estimated, the center of the recto patch and the shifted center of the verso patch are taken as a pair of geometrically corresponding locations, whose coordinates will be used to estimate the coefficients of the projective matrix.

To detect the patches, a square window is simultaneously moved across the two sides in such a way to span the whole image domain. The moving step may have a size smaller than the window size, to increase the number of detected corresponding points. According to the requested properties, the pairs of regions that are good candidates to be used for robustly estimating their relative displacements are those that both contain some text (either see-through in one side and foreground in the opposite side, or mixed see-through and foreground in both sides), and pure background regions, i.e. regions with small values of standard deviation, are discarded. On average, with this criterion, we are able to locate a large number of patch pairs, equally distributed across the image. This condition is very important to capture the different displacements caused by a projective transformation in the different areas of the image.

The procedure above is depicted in Figures 1 and 2. Figure 1 shows the recto-verso misaligned sides of a manuscript, where four pairs of useful patches, out of the many selected, are highlighted and identified with letters A, B, C and D. In Figure 2 the four patches are shown enlarged and paired (recto on the left and verso on the right). The white crosses indicate the central point of the recto and the corresponding point in the verso, found through the cross power spectrum of the two patches.

In general, a single application of the registration procedure suffices to obtain a satisfactory alignment of the two sides. However, when the deformation is significant, it might happens that, in some areas of the image, the two patches do not share any common pattern, so that the computed displacement is wrong and meaningless. This, obviously, affects the accuracy of the estimated transformation coefficients. Thus, it may be necessary to iterate the procedure, until some measure of similarity between the two images, such as the mutual information, stabilizes. In all our experiments, less than

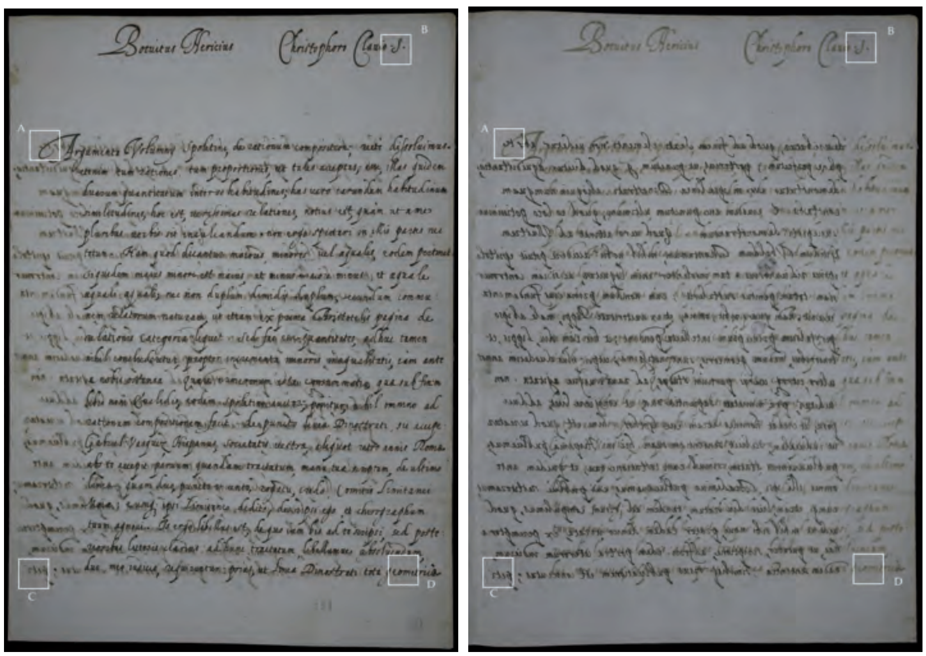

(a) (b)

Figure 1: The mechanism to detect pairs of corresponding points - selection of the patches: (a) recto with four patches highlighted; (b) the four patches at the same position in the misaligned, mirrored verso.

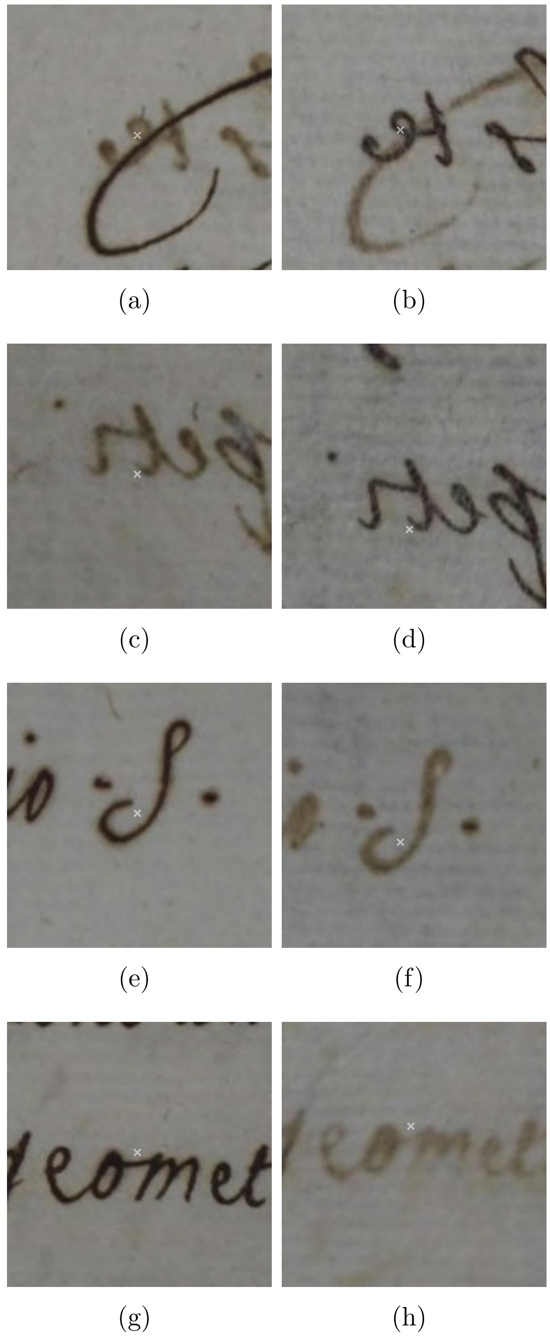

Figure 2: Corresponding points detected via cross power spectrum of the four pairs of patches highlighted in Figure 1: (a) and (b) patches A; (c) and (d) patches B; (e) and (f) patches C;(g) and (h) patches D.

10 iterations were sufficient.

When the manuscript is acquired through a multispectral camera, we already mentioned that it is likely that the three channels of each single side appear misaligned, as shown in Figure 3(a), where a detail of a manuscript recto is shown. Consequently, the misalignment of the mirrored color planes of the verso is “inverted” (see Figure 3(b)). To correct the color shift and geometrically register the two sides, we start correcting the color misalignment of the RGB recto (Figure 3(c)). This is trivial if, disregarding possible different resolutions of the three color filters, we assume the color shift only caused by global displacements between the three channels. Hence, choosing a reference channel, the relative displacements of the other two channels can be computed still via the shift property of the FT, by using a single pair of patches. Subsequently, we separately estimate and apply as described before the individual projective transformations from each channel of the color corrected recto and the homologous channel of the acquired verso. The final result is shown in Figure 3(d). It is apparent that in the registered verso the correct RGB appearance has been restored as well.

3 The restoration method

The algorithm to remove bleed-through from registered RGB recto-verso pairs is the automatic version of the one we proposed in [16], here separately applied to each pairs of homologous color planes. Since this algorithm acts at the level of the individual pixel, it also represents a way to validate the performance of the registration algorithm. The images are modeled through the following non-stationary, linear convolutional model:

$$\begin{aligned} D_r^{c,obs}(t) &= D_r^c(t) + q_v^c(t)\,[h_v^c(t) \otimes D_v^c(t)] \\ D_v^{c,obs}(t) &= D_v^c(t) + q_r^c(t)\,[h_r^c(t) \otimes D_r^c(t)] \\ t = 1, 2, &\ldots, \mathrm{T}, \quad c = R, G, B \end{aligned} \tag{5}$$

with

$$D^c(t) = -log\left(\frac{s^c(t)}{R^c}\right) \tag{6}$$

where $D_r^{c,obs}(t)$ and $D_v^{c,obs}(t)$ are the observed optical densities, and $D_r^c(t)$ and $D_v^c(t)$ are the unknown, ideal ones, of the front and back side, respectively, at channel c and pixel t. Each density is related to the corresponding

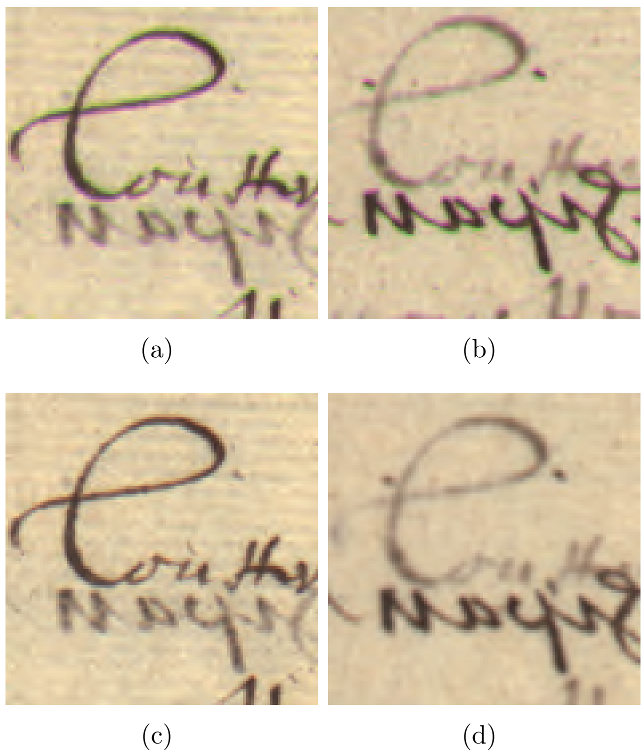

Figure 3: Alignment of a recto-verso manuscript acquired with a multispectral camera - a detail: (a) recto; (b) verso; (c) color corrected recto; (d) verso aligned on the color corrected recto.

reflectance s^c through eq. (6), involving a suitable constant R^c that represents, in the two instances R_r^c and R_v^c, the mean reflectance of the recto and verso background. The model includes two unit volume Point Spread Functions (PSF), h_r^c and h_v^c, describing the smearing of ink that penetrates or shines through the paper, thus allowing a pattern in a side to match the corresponding one in the opposite side. These PSFs are stationary throughout the image, but characterized by different gains $q_r^c(t)$ and $q_v^c(t)$, which have the physical meaning of interference levels from the front to the back and viceversa, at each pixel.

Eqs. (5) define 3 independent systems of equations. Thus, let us consider, from now on, just one of such systems, and, for simplicity of notation, drop the dependence on the specific channel c.

To invert this system, the model parameters R_r and R_v, $q_r(t)$ and $q_v(t)$, $\forall t$, and h_r and h_v, must be known. Taking advantage of the preliminary registration step, R_r and R_v are estimated as the intensity averages within the detected pure background patches. We assume that both h_r and h_v have the form of a centered, Gaussian function, whose size and standard deviation can be approximately estimated from the extent of the character smearing in the bleed-through pattern.

To estimate $q_r(t)$ and $q_v(t)$ at each pixel t, we first apply the following formulas:

$$\begin{aligned} q_r(t) &= \frac{D_v^{obs}(t)}{h_r(t) \otimes D_r^{obs}(t) + \epsilon} \\ q_v(t) &= \frac{D_r^{obs}(t)}{h_v(t) \otimes D_v^{obs}(t) + \epsilon} \end{aligned} \tag{7}$$

where ϵ is a small positive constant to avoid indeterminacies or infinity.

It is apparent that eqs. (7) make both sense only when the ideal density is zero (i.e. background in both sides), also automatically returning null interference levels that allow the reconstructed images to retain there the observed values. For pixels of foreground in one side and see-through in the opposite side $q_r(t)$ and $q_v(t)$ should be mutually exclusive, that is $q_v(t) > 0$, $q_r(t) = 0$ or $q_v(t) = 0$, $q_r(t) > 0$. In practice, since only one of the two equations makes sense, we will obtain $q_r(t) > q_v(t) > 0$ when the first of eqs. (7) does not hold true, and $q_v(t) > q_r(t) > 0$ otherwise. Assuming interferences less dark than the foreground, the two cases are discriminated maintaining the smallest between the two computed interference levels, and setting the other to zero. In the occlusion pixels none of the two equations (7) hold true, and give overestimated interference levels, causing the "cancellation" of the occlusion pixels in one of the two sides. Provided that the two inks reflect similarly under the same wavelength, we can expect that the observed densities at the occlusions are the highest across the manuscript and close to each other, so that they can be located with the aid of suitable thresholds, and then the two interference levels set both to zero.

Once the model parameters are known, D_r and D_v are computed through the following single step:

$$\begin{aligned} D_r(t) &= D_r^{obs}(t) - q_v(t)\left[h_v(t) \otimes D_v^{obs}(t)\right] \\ D_v(t) &= D_v^{obs}(t) - q_r(t)\left[h_r(t) \otimes D_r(t)\right] \end{aligned} \tag{8}$$

More details can be found in [16], where this algorithm has been applied to grayscale documents.

4 Experimental results

We present here some results of our experimentation on several recto-verso pairs of color manuscripts, acquired either with a CCD camera or with a multispectral camera.

We first present the results of the registration method. In Figures 4(a)-(c), the original recto and verso of a 4356×3072 manuscript are shown, along with their superpositions in transparency, showing a significant misalignment. Figure 4(d) shows the superposition of the original recto with the verso registered by our procedure. To obtain this result, approximately 4400 pairs of 101×101 patches were selected, and the registration algorithm was iterated in order to reach stabilization of the following measure of Normalized Mutual Information (NMI):

$$NMI(r,v) = \frac{MI(r,v)}{\sqrt{H(r) \times H(v)}} \tag{9}$$

where $MI(r,v)$ is the Mutual Information between the original recto r and the registered verso v:

$$MI(r,v) = H(r) + H(v) - H(r,v) \tag{10}$$

and H is the entropy. For this experiment, the NMI becomes stable after 5 iterations, with a typical increasing behaviour.

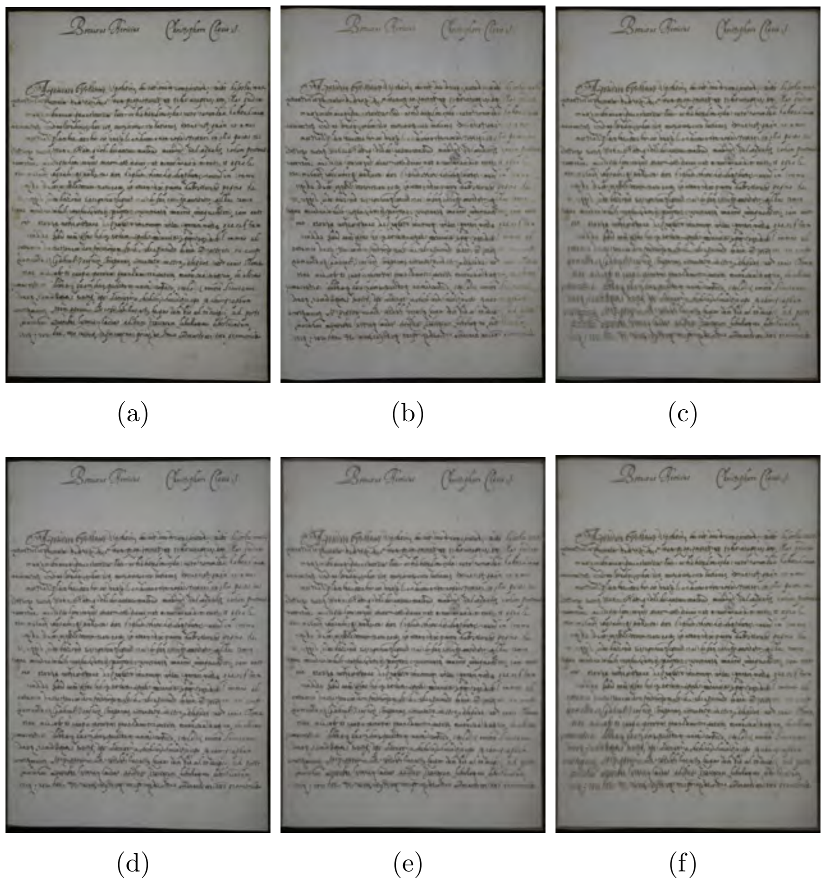

Figure 4: Alignment of a recto-verso manuscript acquired through a CCD camera: (a) original recto; (b) original verso; (c) superposition in transparency of the two sides; (d) superposition of the two sides after projective registration with our method; (e) superposition of the two sides after affine registration with our method; (f) superposition of the two sides after affine registration based on Fourier-Mellin. Original images (a) and (b): reproduction by courtesy of The Historical Archive of the Pontificia Università Gregoriana, APUG 529, c. 134r/v (Fondo Clavius).

Matrix P of the projective transformation, obtained by composing the sequence of the matrices at each iteration, was:

$$P = \begin{bmatrix} 0.969 & -0.016 & -1.071e-05 \\ -0.002 & 0.983 & 3.621e-07 \\ 16.181 & 19.539 & 0.999 \end{bmatrix} \quad (11)$$

By directly applying this matrix to the original misaligned verso, we obtained the same registered image and a very similar value of NMI. By using the same set of corresponding points, but estimating with our method the matrix of an affine transformation, after 5 iterations the NMI was stable but at a lower value. The superposition of the registered verso with the original recto is shown in Figure 4(e). Finally, Figure 4(f) shows the superposition of the original recto with the verso registered with an affine registration algorithm based on the Fourier-Mellin transformation [23]. The value of the NMI was the same obtained when the affine registration is performed with our method.

Looking at both Figure 4(e) and Figure 4(f) it is possible to note that the affine registrations worked quite well in the central part of the images, whereas they performed very poorly at the corners.

Once the recto-verso pairs have been registered, and, when necessary, the color corrected, we apply the restoration algorithm to each pair of color channels, and then obtain the final result by recomposing the restored color channels for each manuscript side. As already mentioned, the mean background value R for computing the optical density is automatically furnished by the preliminary registration algorithm. As PSF, for all the experiments shown below, we used the same Gaussian function, of size 11×11 and standard deviation $\sigma = 3$.

For the recto-verso pair of Figures 4 (a) and (b), the results of restoration, after registration with our method, are shown in Figures 5 (c) and (d) for a detail, to better appreciate the satisfactory removal of the interferences, while preserving the occlusion areas and the paper color and texture. Since this detail has been selected in the central part of the images, its restoration after affine registration was satisfactory as well.

We then selected another detail, picked up in the bottom left part of the images. The original verso is shown in Figure 6(a), whereas Figure 6(b) shows the result of restoration when registration is performed with our method. Figures 6(c) and (d) show the verso registered with the method based on Fourier-Mellin and the verso registered with our method, respectively, with

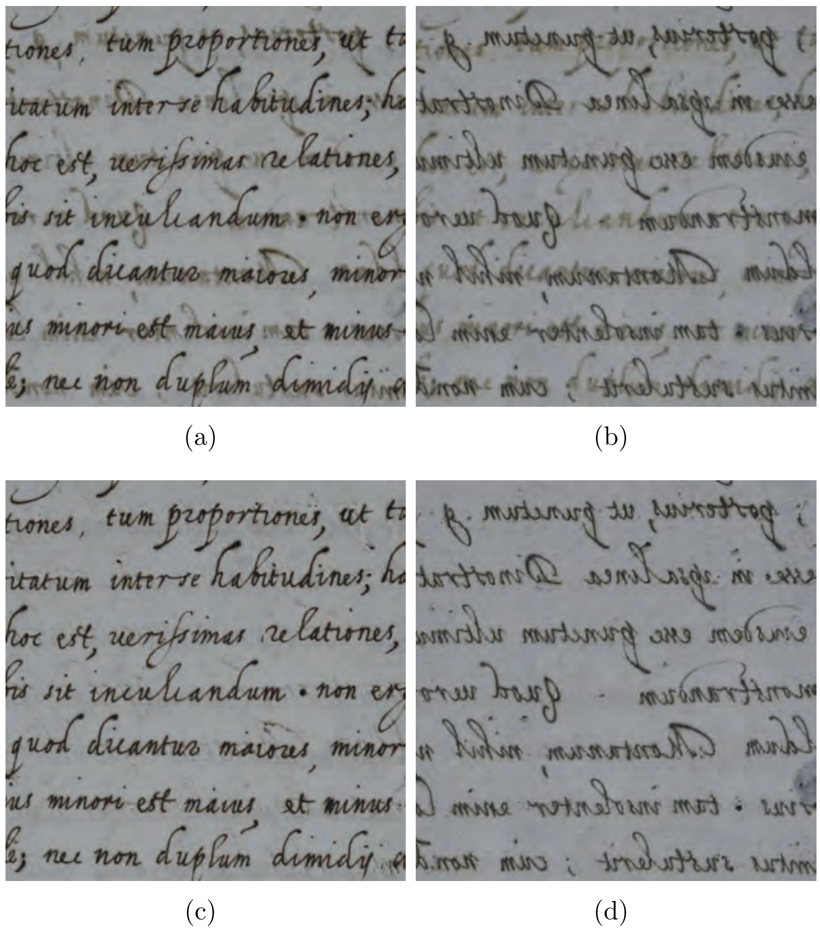

Figure 5: Restoration of the registered recto-verso pair of Figure 4 (a) and (b): (a) a detail of the recto; (b) corresponding detail of the registered verso; (c) corresponding detail of the restored recto; (d) corresponding detail of the restored verso.

superimposed in red the maps of the non-zero q_r values computed by the restoration algorithm. It is apparent the noticeable mismatch between the red pattern and the interferences to be removed when the affine registration is applied, whereas the match is almost exact when the projective registration is used. This means that the restoration of the recto-verso pair registered through the affine transformation would leave, at best, the images unaltered, with also the possibility that some parts of the foreground would be removed in place of the interferences.

The subsequent Figure 7 shows the results of alignment and then restoration of another manuscript. Note that restoration is able to remove almost all the unwanted interferences, even if very inhomogeneous in intensity. Conversely, all the marks genuinely belonging to the manuscript, which carry on information possibly useful to the scholars, have been preserved (i.e., the marks left on the paper by the manuscript folding, the stamp in its original color, and the pencil annotations at the top of the recto).

In the experiment of Figure 8 we performed color correction, alignment, and then restoration of a manuscript acquired with a multispectral camera. The performance of the procedure is comparable to the previous experiments. We however recognize that some annoying single-color “imprints” of the removed interferences are still visible in the restored images, due to the inhomogeneity of the background. However, since we know where see-through was located, this effect could be corrected through inpainting with suitable patterns extracted from the background texture, as done, e.g., in [3].

The example images processed for this work can be obtained upon request.

5 Performance evaluation

The registration algorithm was implemented in Matlab R2014 on a portable computer with an Intel Core i7 2.9 GHz processor.

Table 1 shows the CPU execution times needed to register 6 pairs of images of different size, content, and degree of misalignment. These CPU times range from 3.8 sec. to 22.5 sec., and do not merely depend on the image size. Rather, they are related to the different image characteristics, e.g. amount of text with respect to background, which influences the number of patches used, and number of iterations. For example, Img_5 is registered in 3.8 sec. even if it is larger than Img_1, which requires 22.5 sec. However, in all

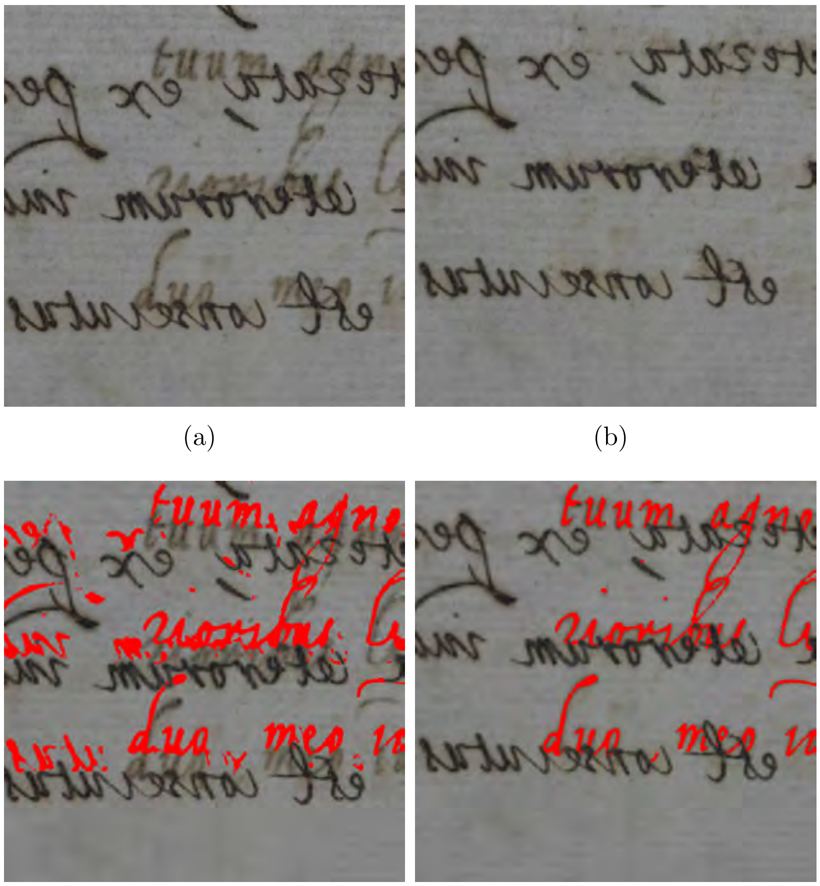

(a) (b) (c) (d)

Figure 6: Restoration of a detail of the verso, after affine and projective registration of the recto-verso pair of Figures 4 (a) and (b): (a) original detail in the bottom-left part of the image; (b) detail restored after projective registration; (c) map in red of the non-zero q_r values after affine registration; (d) map in red of the non-zero q_r values after projective registration.

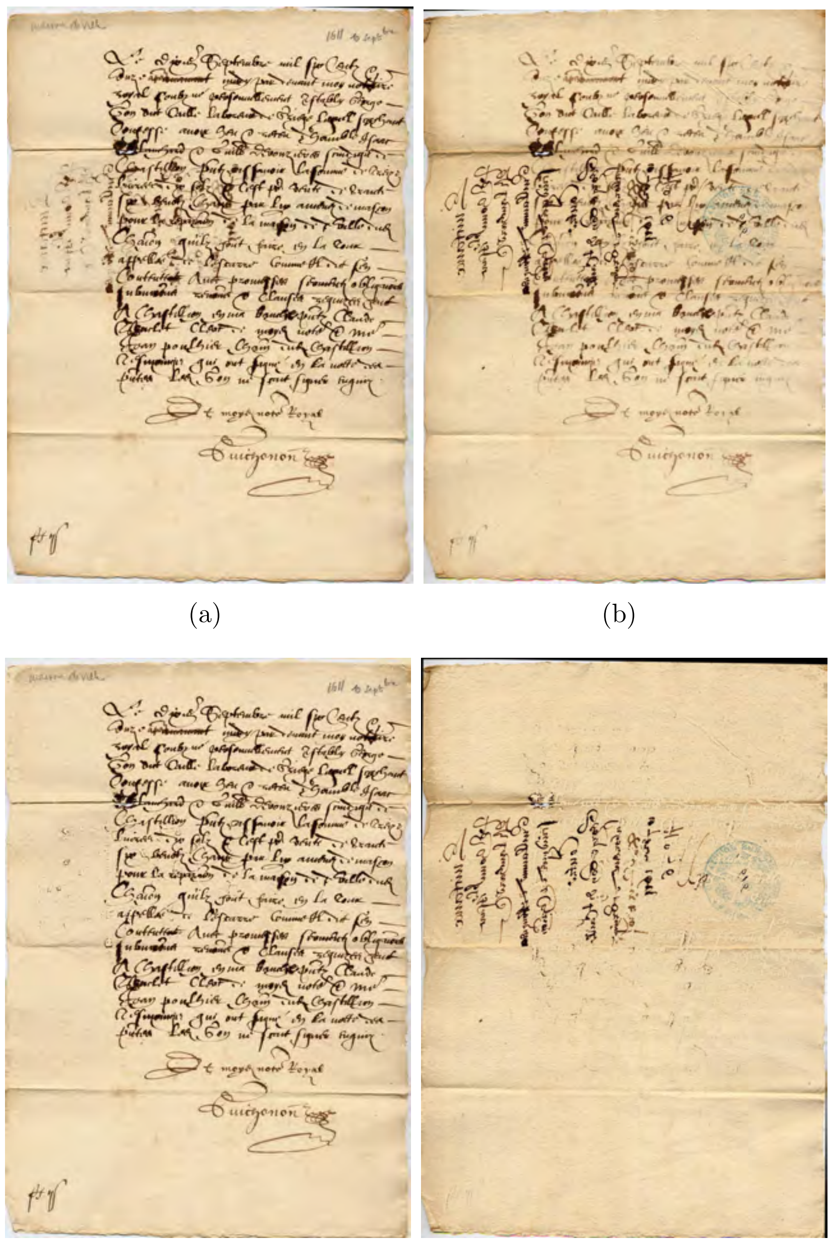

Figure 7: Registration and restoration of a recto-verso manuscript: (a) original recto; (b) original verso; (c) restored recto; (d) registered and restored verso.

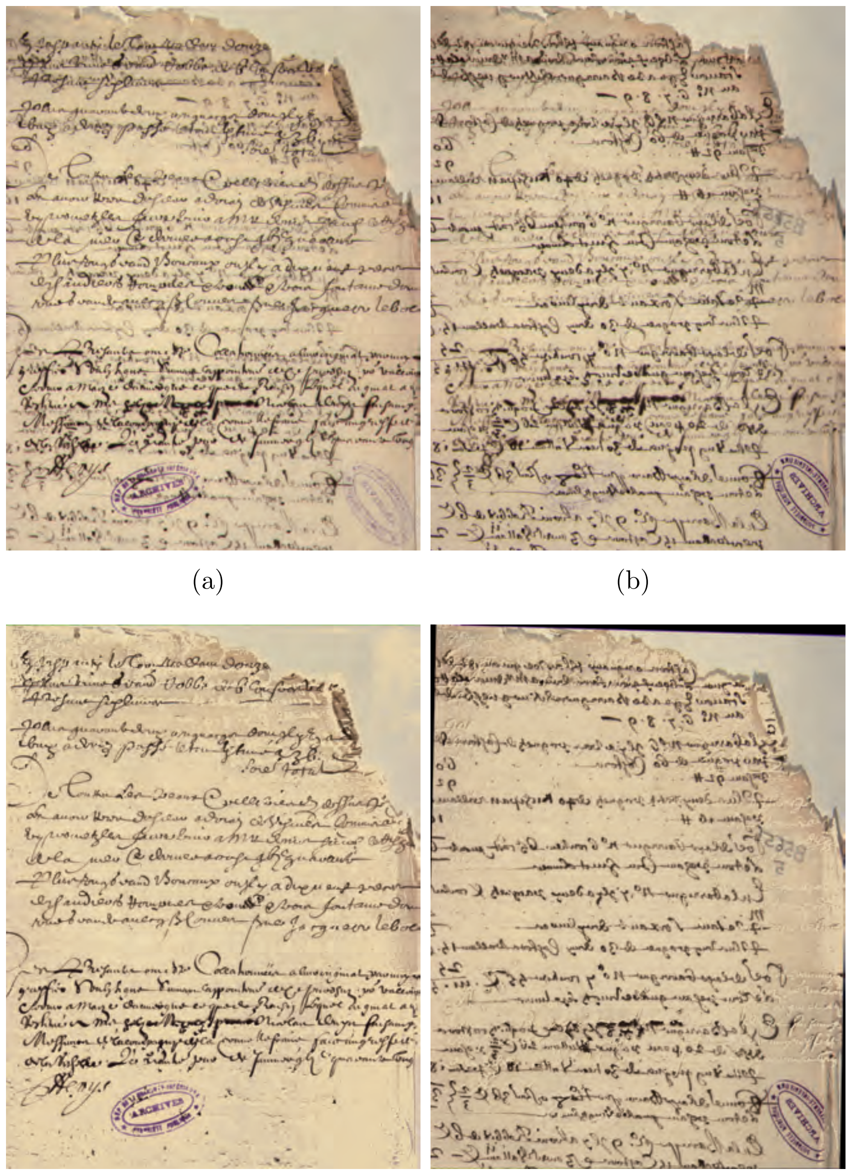

(a) (b) (c) (d)

Figure 8: Correction of the color, registration and restoration of a recto-verso manuscript: (a) original recto; (b) original verso; (c) restored recto; (d) registered and restored verso.

Table 1: Registration execution time

	Img_1		Img_2		Img_3	
rows x cols	2768	4020	2694	3882	3114	4416
M pixels	11.1		10.5		13.8	
Exec. time (sec.)	22.51		12.79		14.04	

	Img_4		Img_5		Img_6	
rows x cols	3066	4362	3044	4323	1036	1360
M pixels	13.4		13.2		1.4	
Exec. time (sec.)	13.77		3.8		6.33	

cases, the execution times are acceptable for this application, and significant improvements could be achieved by implementing the algorithm in a compiled programming language, such as C++.

As per the algorithm scalability, we assumed that all subparts of a same image exhibit approximately the same behavior, and selected, for each image, different subparts of different sizes. As shown in Figure 9, for all the 6 images considered the registration time is approximately linear with the subpart size.

We repeated the same experiment (not shown here) by using all image patches without discarding those containing only background in one side. The scalability behavior is still linear with size, though the execution times are approximately three times higher, and a higher number of iterations is also needed. However, the quality of registration, estimated through the NMI, is the same.

6 Conclusion

We described an automatic and fast procedure for registration and digital restoration of color images of recto-verso pairs of ancient manuscripts, degraded by bleed-through.

We assumed flat manuscripts but considered the rigid deformation between the two sides to be a projective transformation, which is frequent due to accidental movements of the camera. Our registration algorithm can also be applied for aligning multispectral acquisitions (e.g., outside the visible range) of either a single side or both sides of a manuscript, and a simplified

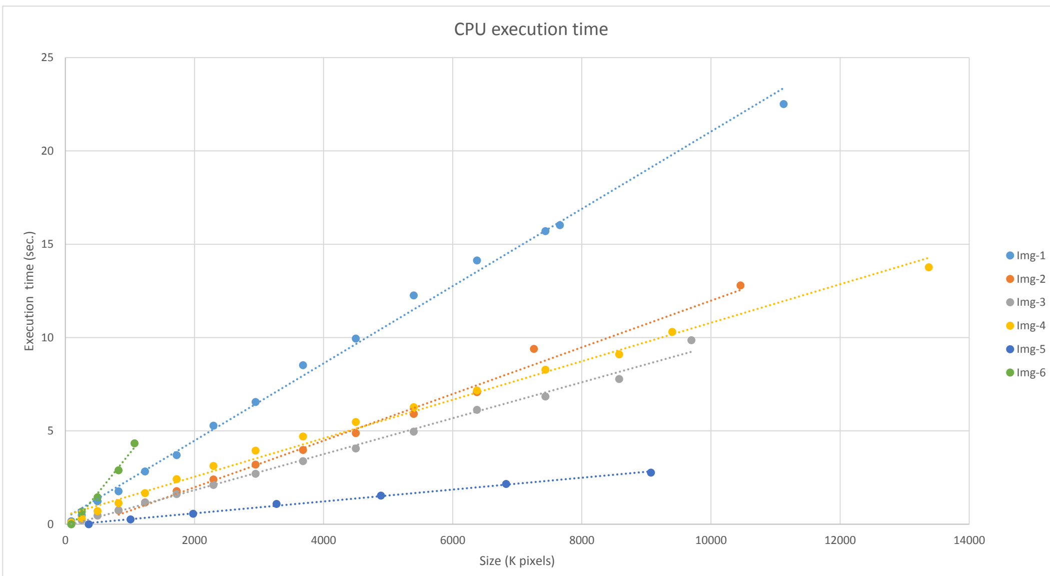

Figure 9: Execution time (in sec.) versus subpart size (in K pixels) for six images.

version can be used to align the color channels of manuscripts acquired with multispectral cameras, where, usually, a mutual shift among them produces a visibly unappealing alteration of the color of the text.

The subsequent restoration algorithm allows for an often very satisfactory removal of the unwanted, uninformative interferences, while leaving unaltered the original appearance of the manuscript, such as color and textures of the paper, stamps, annotations, and all other aging marks. Furthermore, since the algorithm acts at the single pixel level, it also constitutes an implicit way to validate the registration quality.

Future improvements regard the extension of the registration algorithm to non-rigid transformations, to cope with folding and curvature of the page, when the manuscript is part of a book, for instance. Other issues, related to restoration, regard relaxing the assumption of interference density lower than foreground density, using inpainting to attenuate the "imprints" sometimes appearing in correspondence of the removed bleed-through pattern, and finding strategies for a more accurate selection of the model parameters at the occlusions. These latter could range from the iterative refining of an initial, rough estimate, to the inclusions of priors on the ideal images.

7 Acknowledgements

This work has been supported by program POR Calabria FESR 2007-2013 - PIA Regione Calabria Pacchetti Integrati di Agevolazione Industria Artigianato Servizi, project ITACA (Innovative Tools for cultural heritage ArChiving and restorAtion).

References

[1] Hanasusanto, G.A., Wu, Z., Brown, M.S.: Ink-bleed reduction using functional minimization. In: The Twenty-Third IEEE Conference on Computer Vision and Pattern Recognition, CVPR 2010, San Francisco, CA, USA, 13-18 June 2010. (2010) 825–832

[2] Huang, Y., Brown, M.S., Xu, D.: User-assisted ink-bleed reduction. IEEE Transactions on Image Processing **19**(10) (2010) 2646–2658

[3] Rowley-Brooke, R., Pitié, F., Kokaram, A.C.: A non-parametric framework for document bleed-through removal. In: 2013 IEEE Conference on Computer Vision and Pattern Recognition, Portland, OR, USA, June 23-28, 2013. (2013) 2954–2960

[4] Tonazzini, A., Bedini, L., Salerno, E.: Independent component analysis for document restoration. IJDAR **7**(1) (2004) 17–27

[5] Tonazzini, A., Salerno, E., Bedini, L.: Fast correction of bleed-through distortion in grayscale documents by a blind source separation technique. IJDAR **10**(1) (2007) 17–25

[6] Tonazzini, A., Gerace, I., Martinelli, F.: Multichannel blind separation and deconvolution of images for document analysis. IEEE Transactions on Image Processing **19**(4) (2010) 912–925

[7] Rowley-Brooke, R., Kokaram, A.C.: Bleed-through removal in degraded documents. In: Document Recognition and Retrieval XIX - DRR 2012, 19th Document Recognition and Retrieval Conference, part of the IS&T-SPIE Electronic Imaging Symposium, Burlingame, California, USA, January 25, 2012, Proceedings. (2012)

[8] Merrikh-Bayat, F., Babaie-Zadeh, M., Jutten, C.: Using non-negative matrix factorization for removing show-through. In: Latent Variable Analysis and Signal Separation - 9th International Conference, LVA/ICA 2010, St. Malo, France, September 27-30, 2010. Proceedings. (2010) 482–489

[9] Sharma, G.: Show-through cancellation in scans of duplex printed documents. IEEE Transactions on Image Processing **10**(5) (2001) 736–754

[10] Ophir, B., Malah, D.: Show-through cancellation in scanned images using blind source separation techniques. In: Proceedings of the International Conference on Image Processing, ICIP 2007, September 16-19, 2007, San Antonio, Texas, USA. (2007) 233–236

[11] Martinelli, F., Salerno, E., Gerace, I., Tonazzini, A.: Nonlinear model and constrained ML for removing back-to-front interferences from recto-verso documents. Pattern Recognition **45**(1) (2012) 596–605

[12] Salerno, E., Martinelli, F., Tonazzini, A.: Nonlinear model identification and seethrough cancellation from recto-verso data. IJDAR, published online 17 March 2012 (2012)

[13] Merrikh-Bayat, F., Babaie-Zadeh, M., Jutten, C.: Linear-quadratic blind source separating structure for removing show-through in scanned documents. IJDAR **14**(4) (2011) 319–333

[14] Almeida, M.S.C., Almeida, L.B.: Nonlinear separation of show-through image mixtures using a physical model trained with ICA. Signal Processing **92**(4) (2012) 872–884

[15] Moghaddam, R.F., Cheriet, M.: A variational approach to degraded document enhancement. IEEE Trans. Pattern Anal. Mach. Intell. **32**(8) (2010) 1347–1361

[16] Tonazzini, A., Savino, P., Salerno, E.: A non-stationary density model to separate overlapped texts in degraded documents. Signal, Image and Video Processing (published online: 13 December 2014 2014)

[17] Zitová, B., Flusser, J.: Image registration methods: a survey. Image Vision Comput. **21**(11) (2003) 977–1000

[18] Pluim, J.P.W., Maintz, J.B.A., Viergever, M.A.: Mutual information based registration of medical images: A survey. IEEE Trans. Med. Imaging **22**(8) (2003) 986–1004

[19] Dubois, E., Pathak, A.: Reduction of bleed-through in scanned manuscript documents. In: PICS 2001: Image Processing, Image Quality, Image Capture, Systems Conference, Montréal, Quebec, Canada, April 22-25, 2001. (2001) 177–180

[20] Wang, Q., Tan, C.L.: Matching of double-sided document images to remove interference. In: 2001 IEEE Computer Society Conference on Computer Vision and Pattern Recognition (CVPR 2001), with CD-ROM, 8-14 December 2001, Kauai, HI, USA. (2001) 1084–1089

[21] Murtagh, F.: A new approach to point-pattern matching. Astronomical Society of the Pacific **104** (April 1992) 301–307

[22] Wang, J., Brown, M.S., Tan, C.L.: Accurate alignment of double-sided manuscripts for bleed-through removal. In: The Eighth IAPR International Workshop on Document Analysis Systems, DAS 2008, September 16-19, 2008, Nara, Japan. (2008) 69–75

[23] Tonazzini, A., Bianco, G., Salerno, E.: Registration and enhancement of double-sided degraded manuscripts acquired in multispectral modality. In: 10th International Conference on Document Analysis and Recognition, ICDAR 2009, Barcelona, Spain, 26-29 July 2009. (2009) 546–550

[24] Rabeux, V., Journet, N., Domenger, J.: Document recto-verso registration using a dynamic time warping algorithm. In: 2011 International Conference on Document Analysis and Recognition, ICDAR 2011, Beijing, China, September 18-21, 2011. (2011) 1230–1234

[25] Li, B., Wang, W., Ye, H.: Multi-sensor image registration based on algebraic projective invariants. Optics express **21**(8) (April 2013) 9824–9838

[26] Wang, J., Tan, C.L.: Non-rigid registration and restoration of double-sided historical manuscripts. In: 2011 International Conference on Document Analysis and Recognition, ICDAR 2011, Beijing, China, September 18-21, 2011. (2011) 1374–1378

[27] Myronenko, A., Song, X.B.: Intensity-based image registration by minimizing residual complexity. IEEE Trans. Med. Imaging **29**(11) (2010) 1882–1891

[28] Rowley-Brooke, R., Pitié, F., Kokaram, A.C.: Nonrigid recto-verso registration using page outline structure and content preserving warps. In: Proceedings of the 2nd International Workshop on Historical Document Imaging and Processing, ACM (2013) 8–13